Carbohydrate Research 379 (2013) 68–77

Contents lists available at SciVerse ScienceDirect

Carbohydrate Research

journal homepage: www.elsevier.com/locate/carres

Synthesis, surface properties, and biocompatibility of 1,2,3-triazole-containing alkyl β-D-xylopyranoside surfactants

E. Davis Oldham [a], Srivenu Seelam [b], Carolina Lema [c], Renato J. Aguilera [c], Jennifer Fiegel [d,e], Stephen E. Rankin [b], Barbara L. Knutson [b], Hans-Joachim Lehmler [a,f,*]

[a] Department of Occupational and Environmental Health, The University of Iowa, UI Research Park, IREH, Iowa City, IA 52242-5000, USA
[b] Department of Chemical and Materials Engineering, University of Kentucky, Lexington, KY 40506, USA
[c] Department of Biological Sciences, Biosciences Research Building, University of Texas at El Paso, 500 West University Ave., El Paso, TX 79968, USA
[d] Department of Pharmaceutical Sciences and Experimental Therapeutics, College of Pharmacy, University of Iowa, Iowa City, IA 52242,USA
[e] Department of Chemical and Biochemical Engineering, College of Engineering, University of Iowa, Iowa City, IA 52242, USA
[f] Interdisciplinary Graduate Program in Human Toxicology, University of Iowa, Iowa City, IA 52242, USA

ARTICLE INFO

Article history:
Received 26 March 2013
Received in revised form 17 June 2013
Accepted 20 June 2013
Available online 28 June 2013

Keywords:
Click chemistry
Huisgen cycloaddition
Carbohydrate surfactants
Langmuir monolayers
Cytotoxicity

ABSTRACT

We are interested in the development of surfactants derived from hemicellulosic biomass, as they are potential components in pharmaceuticals, personal care products, and other detergents. Such surfactants should exhibit low toxicity in mammalian cells. In this study we synthesized a series of alkyl or fluoroalkyl β-xylopyranosides from azides and an alkyne using the copper-catalyzed azide-alkyne (CuAAC) 'click' reaction in 4 steps from xylose. The purified products were evaluated for both their surfactant properties, and for their biocompatibility. Unlike other carbohydrate-based surfactants, liquid–crystalline behavior was not observed by differential scanning calorimetry. The triazole-containing β-xylopyranosides with short (6 carbons) and long (>12 carbons) chains exhibited no toxicity at concentrations ranging from 1 to 1000 μM. Triazole-containing β-xylopyranosides with 8, 10, or 12 carbons caused toxicity via apoptosis, with CC_{50} values ranging from 26–890 μM. The two longest chain compounds did form stable monolayers at the air–water interface over a range of temperatures, although a brief transition to an the unstable monolayer was observed.

1. Introduction

The broad range of commercial applications of surfactants has increased the need for ones that are biologically safe.[1] As the demand continues to grow, the importance of surfactants derived from renewable resources has risen. Carbohydrate-based surfactants often satisfy requirements of low toxicity and sustainable production, and have been used as pharmaceuticals, detergents, agrochemicals, and personal care products.[1] The most readily available carbohydrates are glucose and xylose, which, together with lignin, are the components of lignocellulose. Recent advancements in the field have allowed for the use of materials derived from cellulose (glucose) and hemicellulose (glucose and xylose).[2] The carbohydrate precursors are readily produced using environmentally friendly processes.[3,4] Additionally, carbohydrate-based surfactants often have low toxicities and can be biodegradable.

The synthesis and physiochemical characterization of xylose-based surfactants have been reported in the literature.[5–7] These surfactants were typically synthesized by enzymatic or Fischer glycosylation reactions, or by hydrolysis of oligosaccharides. The products, which were unspecified mixtures of anomers, exhibited typical chemical properties of surfactants. Previously we have synthesized β-alkyl xylopyranosides as novel surfactants which exhibited liquid–crystalline behavior and low in vitro toxicity.[8] To further expand the available structures of carbohydrate-based surfactants, we are interested in designing surfactants with linkers connecting the carbohydrate head group to the hydrophobic tail, allowing the rapid synthesis of diverse surfactants with different hydrophobic tails. Here we chose the 1,2,3-triazole, a heterocyclic moiety readily synthesized by a copper-catalyzed 'click' reaction between an azide and an alkyne, as a versatile linker. This heterocycle has found widespread usage[9] in a broad range of disciplines such as medicinal chemistry and materials chemistry. The 1,2,3-triazole moiety has been found in bolaamphiphile,[10] star-like,[11] and fluorocarbon surfactants.[12,13] While both xylose head groups and 1,2,3-triazoles have been used in surfactants, the two have

* Corresponding author. Tel.: +1 (319) 335 4310; fax: +1 (319) 335 4290.
E-mail address: hans-joachim-lehmler@uiowa.edu (H.-J. Lehmler).

0008-6215/$ - see front matter © 2013 Elsevier Ltd. All rights reserved.
http://dx.doi.org/10.1016/j.carres.2013.06.020

not been used in combination. Triazole-linked glucose-based surfactants have been synthesized previously either by the copper-catalyzed azide alkyne cycloaddition (CuAAC) reaction of a glycosyl azide and a propargylated fatty alcohol or a propargylated sugar and an alkyl azide.[14–17] In this paper we report the synthesis and characterization of physiochemical properties of xylose-based carbohydrates containing a triazole linker as well as a preliminary biocompatibility assessment.

2. Results and discussion

2.1. Synthesis of triazole-linked alkyl xylosides

We sought an efficient route to xylose surfactants containing hydrophobic chains of variable length linked to the polar head group with a 1,2,3-triazole generated by a 'click' reaction. This copper-catalyzed reaction of azides and alkynes proceeds under mild conditions with excellent regiochemistry; many functional and protection groups are tolerated.[18] Furthermore, this 'click' reaction allows for short, straight-forward syntheses, as few functional group interconversions and protecting group manipulations are required. In the context of surfactants, different combinations of polar head groups and hydrophobic tails can be readily synthesized from common precursors.

Triazole-containing surfactants were synthesized in four steps from D-xylose (**1**) as described in Scheme 1; this scheme has been previously used to synthesize glucose-based triazole-containing surfactants.[15] This strategy was chosen to yield anomerically pure surfactants, as previous work has suggested the β-alkyl anomers may be more biocompatible.[19,20] Briefly, D-xylose was peracetylated with sodium acetate in acetic anhydride at 100 °C,[21,22] producing **2** as the β-anomer. Glycosylation with propargyl alcohol under Lewis-acid-promoted conditions afforded **3**[23] as the β-anomer. The CuAAC reaction between **3** and alkyl azides (prepared from the corresponding alkyl bromides or iodides)[24] was carried out using 0.1 equiv $CuSO_4$ and 0.2 equiv sodium ascorbate in aqueous *tert*-butanol[18] to generate **4a–g**. The coupling reaction was typically complete in 1 h, with yields ranging from 64% to 80%. In the last step the acetate protecting groups were removed with sodium methoxide, followed by neutralization with Dowex 50 W × 8–100 ion exchange resin[8] to yield the triazole-linked surfactants **5a–g**.

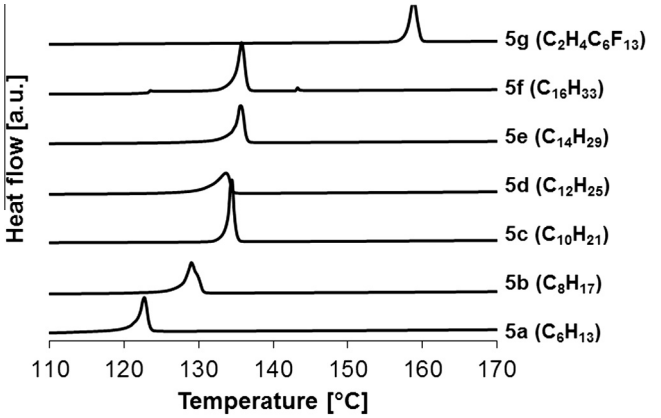

Figure 1. Representative thermograms of **5a–g** obtained by differential scanning calorimetry. Positive peaks indicate endothermic transitions. Only the region of the thermogram with a phase transition is shown. See under Experimental procedures for DSC parameters. The thermograms were plotted with relative heat flow on the *y*-axis in arbitrary units [a.u.].

The final products were purified by recrystallization in 50–73% yield and provided satisfactory elemental analysis. In general, the yield of the final deprotection step increased with increasing chain length.

2.2. Differential scanning calorimetry (DSC) of 5a–g

The phase transitions seen in DSC thermograms give information about thermal stability of compounds. Furthermore, DSC allows a preliminary assessment of liquid–crystalline properties, a common characteristic of surfactants, including synthetic carbohydrate-based surfactants,[25–29] and biological surfactants such as cell membranes.[30] The liquid–crystalline behavior of these surfactants may correlate with their biological activity.[31] The transitions of the triazole-linked surfactants **5a–g** were therefore characterized by differential scanning calorimetry (DSC). For each triazole-containing surfactant a single, endothermic peak was observed, as shown in Figure 1. The phase transitions ranged from 122 to 136 °C and, analogous to the structurally related triazole-containing alkyl β-gluco-

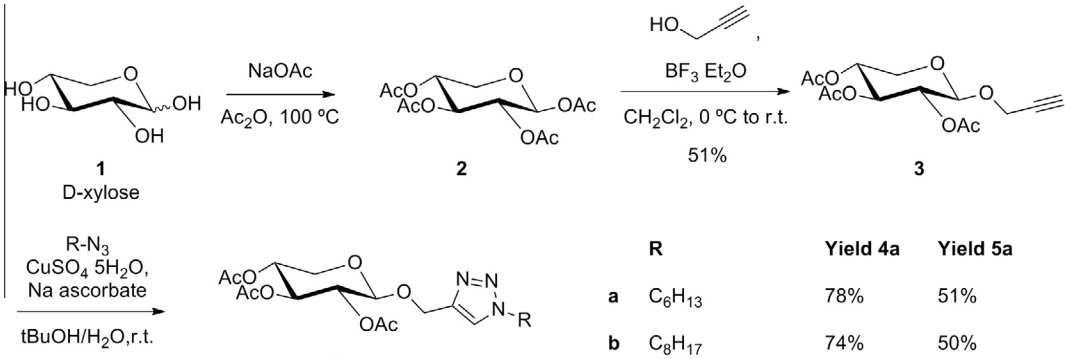

	R	Yield 4a	Yield 5a
a	C_6H_{13}	78%	51%
b	C_8H_{17}	74%	50%
c	$C_{10}H_{21}$	74%	55%
d	$C_{12}H_{25}$	64%	65%
e	$C_{14}H_{29}$	73%	65%
f	$C_{16}H_{33}$	80%	73%
g	$C_2H_4(CF_2)_5CF_3$	77%	56%

Scheme 1. Synthesis of triazole-linked alkyl xylopyranosides via a copper-catalyzed azide alkyne cycloaddition (CuAAC) reaction.

Table 1
Average transition temperature and enthalpy values for **5a–g**, determined by differential scanning calorimetry

Compound	Transition temperature (°C)	Enthalpy (kJ/mol)
5a (C_6H_{13})	120.1 ± 0.8	27 ± 4
5b (C_8H_{17})	126.9 ± 0.8	31 ± 5
5c ($C_{10}H_{21}$)	133.6 ± 0.1	39 ± 2
5d ($C_{12}H_{25}$)	130.1 ± 0.2	34 ± 2
5e ($C_{14}H_{29}$)	134.7 ± 0.4	41 ± 1
5f ($C_{16}H_{33}$)	134.9 ± 0.1	44 ± 2
5g ($C_2H_4C_6F_{13}$)	158.8 ± 0.2	45 ± 1

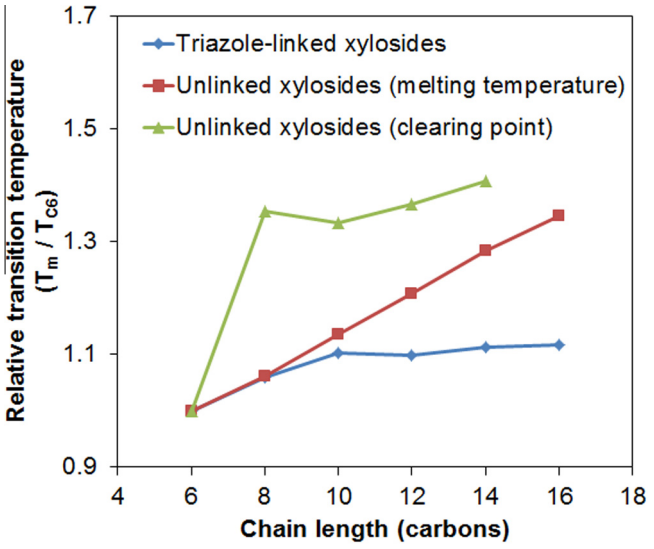

Figure 2. Relative transition temperature (T_m/T_{C6}) of triazole-linked surfactants **5a–f** (blue diamonds) and the corresponding β-alkyl xylopyranosides[8] without the triazole linker (melting temperature: red squares; clearing point: green triangles) observed in the corresponding differential scanning calorimetry thermograms. T_{C6} is the respective transition temperature of the corresponding hexyl derivative. (For interpretation of the references to color in this figure legend, the reader is referred to the web version of this book.)

pyranosides,[15] increased with increasing chain length (Table 1). The partially fluorinated surfactant **5g** melted at 158 °C, which is considerably higher compared to the corresponding hydrocarbon surfactant **5b**. A similar increase in the phase transition temperature of fluorinated surfactants relative to the corresponding hydrocarbon surfactant has been previously observed for alkyl glucopyranosides[19] and xylopyranosides.[8] The phase transition temperature of the hydrocarbon surfactants began to level off at chain lengths $\geqslant$10 carbon atoms (Fig. 2). Similarly, the increase in the phase transition temperature of the structurally analogous triazole-containing alkyl β-glucopyranosides was less pronounced for surfactants with tetradecyl and hexadecyl tails.[15] The enthalpies associated with the phase transition were calculated from integration of the thermograms and ranged from 26.6 kJ/mol to 45.1 kJ/mol; these values followed the same trend as the transition temperature.

In contrast to triazole-linked surfactants **5a–g**, the phase transitions of simple alkyl β-xylopyranosides[8], which contain no triazole linker but otherwise are structurally analogous to **5a–g**, were drastically lower (ranging from 68 to 91 °C) and showed a stronger dependence of melting temperature on tail chain length (Fig. 2). The analog of the partially fluorinated surfactant **5g** also had a significantly lower melting point of 105 °C. The markedly higher phase transition temperatures of the triazole-linked surfactants **5a–g**, relative to simple alkyl xylopyranosides, indicate that the triazole linker stabilizes the solid-state packing. The addition of the triazole linkage[15] appeared to have a comparable effect on the melting points in the case of the structurally related alkyl β-glucopyranosides.[32]

The simple alkyl xylopyranosides with a glycosidic linkage also exhibited liquid–crystalline behavior in DSC thermograms, as evidenced by the presence of a second, smaller peak corresponding to the clearing point in the thermograms.[8] This type of peak has been observed for alkyl glucopyranosides,[33] amide-linked glucopyranosides,[25] and xylitols.[26,34] The previously reported triazole-containing alkyl β-glucopyranosides also exhibited liquid–crystalline properties.[15] However, no second peak indicative of liquid–crystalline behavior was observed in the thermograms of any triazole-containing alkyl β-xylopyranosides **5a–e** and **g**; a small peak possibly representing a clearing point was observed with **5f**. Further work, involving microscopy techniques such as cryo-transmission electron microscopy (cryo-TEM) or polarized optical microscopy, is therefore needed to determine the nature of the thermal transitions of triazole-containing alkyl β-xylopyranosides.

2.3. In vitro cytotoxicity of triazole-containing alkyl xyloside surfactants

Very little is currently known about the toxicity of alkyl glycoside surfactants. The toxicities of alkyl β-D-xylopyranosides, including those containing partially fluorinated hydrophobic tails, have been investigated in mammalian cell lines.[8,19,20,35,36] In the present study the toxicities of the triazole-linked surfactants **5a–g** were investigated in cells in culture using the 3-(4,5-dimethylthiazol-2-yl)-5-(3-carboxymethoxyphenyl)-2-(4-sulfophenyl)-2H-tetrazolium (MTS) assay used previously.[8] Spontaneously immortalized human keratinocytes (HaCaT), Jurkat human T-cell lymphoblastic leukemia cells, and human Hs27 fibroblasts were employed as cell lines in this assay. HaCaT cells model potential effects of toxicants on skin cells;[37] this is particularly relevant for compounds such as surfactants which have potential applications in personal care products. Jurkat cells have typically been used for determining the toxicity of a wide range of compounds with good sensitivity.[38,39] Hs27 cells are often used as a control in comparison to other cancer cell lines.[40] While the triazole unit has been increasingly used in biological applications,[41] it is still important to determine the effect on biocompatibility that the incorporation of this linker into a carbohydrate surfactant would have.

The chain-length dependence of the toxicities of **5a–g** was determined in vitro. Compounds **5a** (hexyl chain), **5e** (tetradecyl chain), **5f** (hexadecyl chain), and **5g** (partially fluorinated side chain) were not toxic in all three cell lines at concentrations ranging from 1 to 1000 μM. The compounds with intermediate chain lengths (**5b–d**), on the other hand, showed moderate toxicity in all three cell lines as assessed using the MTS assay (Fig. 3). CC_{50} values, corresponding to the concentration at which 50% of the cells were viable,[42] were calculated as described in the Experimental procedures section, using the data shown in Figure 3, and are summarized in Table 2. In both Jurkat and HaCaT cells, the toxicity increased as the tail length increased from **5b** to **5d**. Surfactant **5c** was approximately 8-fold more toxic than **5b** in both of these cell lines. Overall, the Jurkat cell line was the most sensitive; **5b–d** exhibited similarly low toxicities in the two non-leukemia cell lines (HaCaT and Hs27).

Interestingly, surfactants **5b** to **5d** had toxicities comparable to alkyl xylopyranosides without the triazole linker.[8] For example, the CC_{50} values of **5b** (containing an octyl side chain) were 890 μM (HaCaT), 694 μM (Hs27), and 580 μM (Jurkat); the corresponding CC_{50} values for ocyl β-xylopyranoside in the previous study were 850, 760, and 460 μM, respectively (Table 2). As in the present study, the intermediate-length alkyl xylopyranosides were also the most toxic. The phenomenon in which surfactants of intermediate lengths

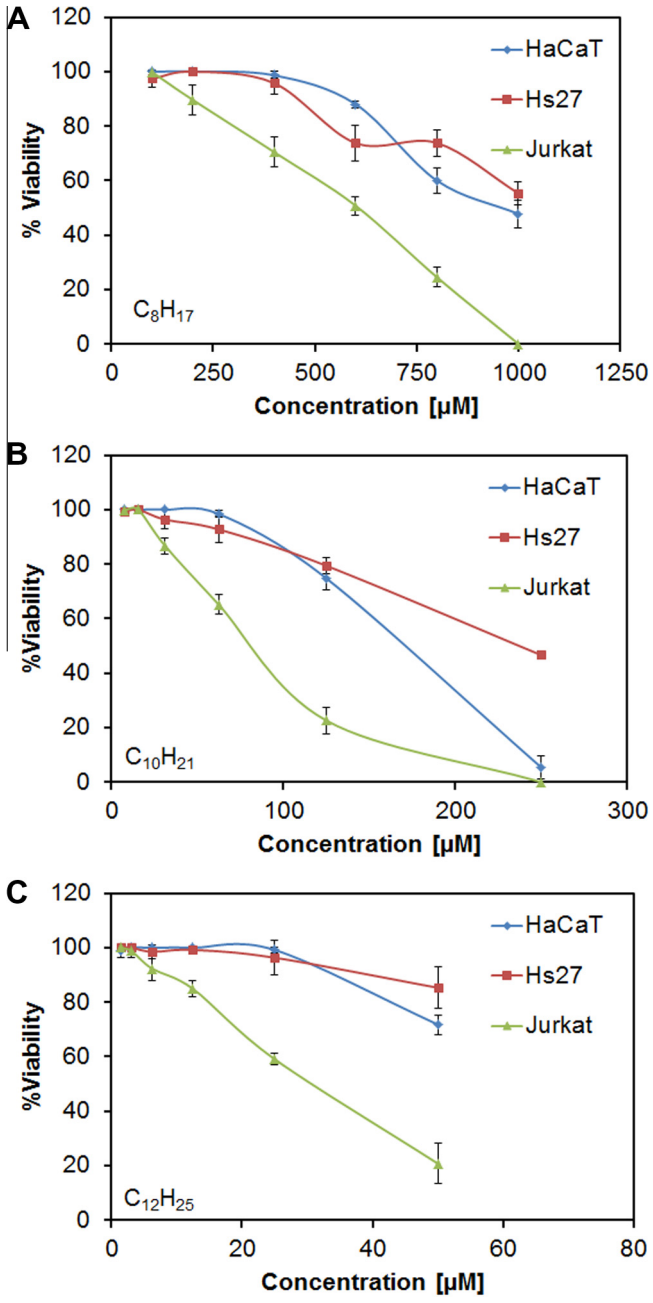

Figure 3. Concentration dependence of cytotoxicity of selected triazoles in HaCaT, Hs27, and Jurkat cells. After 18 h (HaCaT and Hs27 cells) or 16 h (Jurkat cells) of treatment with (A) **5b**, (B) **5c**, or (C) **5d**, MTS was added and incubation continued for 2 h (HaCaT and Hs27 cells) and 4 h (Jurkat cells) before measuring absorbance at 490 nm. Error bars represent the standard deviation of the mean from three replicates. The chain length of the hydrophobic tail is indicated on each panel.

exhibit higher toxicity than those with shorter or longer chains, is known as the 'cut-off' effect;[43] this effect has been seen with carbohydrate surfactants in mammalian cell lines[8,19,20] and bacteria.[44,45] The lack of a linear dependence between chain length and biological activity is at first surprising, if the activity is assumed to be a function of membrane permeability: as the length of the hydrocarbon chain of a surfactant increases, the octanol–water partition coefficient also increases, which should increase membrane partitioning and, ultimately, activity. Thus, the basis of the cut-off effect likely is the result of factors other than membrane partitioning, for example decreasing aqueous and lipid solubility, decreasing critical micelle concentration, increasing binding to proteins in the culture medium or decreasing diffusion through the cell membrane with increasing chain length.[43,46]

Fluorinated surfactants have been shown to be less toxic than the corresponding hydrocarbon surfactants.[47,36,48] In agreement with these earlier studies, the partially fluorinated hydrophobic tail in surfactant **5g** appears to have a protective effect, as **5g** showed no measurable inhibition of cell viability in any cell line in the concentration range studied, which is in contrast to the corresponding hydrocarbon surfactant **5b** in HaCaT or Jurkat cell lines. In some cases, the toxicity of fluorinated surfactants appears to follow a '1.5 rule',[49] which states that each CF_2 approximates 1.5 CH_2 groups. Thus, for **5g**, the 1.5 rule would correspond to 2 CH_2 groups +1.5 × 6 CF_2 groups = 11 CH_2 groups. For example, the CC_{50} values of the non-triazole-linked fluoroalkyl xylopyranoside (163–267 μM) and non-triazole-linked decyl xylopyranoside (123–167 μM) were comparable.[8] In this study, triazole-linked surfactant **5g** does not obey this rule, as the toxicities of **5g** and the structurally analogous surfactant **5c** are not comparable. It is possible that the triazole should be considered part of the side-chain; further separation of the rigid, fluorocarbon chain from the headgroup due to the presence of the triazole likely alters the three-dimensional structure of the surfactant, which would in turn affect interaction with possible biological targets.

To further investigate the mechanisms of toxicity of triazole-linked surfactants, the levels of apoptotic and necrotic cells were determined with annexin V-FITC staining after exposure of Jurkat cells to the triazole-linked xylosides **5b–d**. The relative amounts of viable, necrotic, and apoptotic cells are shown in Figure 4; hydrogen peroxide and Tween-20 were used as positive controls for apoptosis and necrosis, respectively; DMSO was the solvent control. Notably, cell death occurred from apoptosis and not necrosis. Triazole **5b** exhibited a profile comparable with the positive controls for apoptosis, octyl xylopyranoside, and hydrogen peroxide.[50] As the chain increased from 8 carbons (**5b**) to 12 carbons (**5d**), the number of apoptotic cells increased, and the number of viable cells decreased; there was no chain length dependence on the number of necrotic cells. A similar chain-length dependent effect on apoptosis was also seen with the xylopyranosides lacking a triazole linker.[8] Thus the mechanism of cell death likely involves complex signaling pathways; for example, the transmembrane protein Fas[51] has been implicated in the toxicity of perfluoralkyl acids (PFAAs). Other possible targets include the caspase-mediated apoptosis pathway. For example, an ionic liquid, containing an imidazolium headgroup and an octyl side chain, increased reactive oxygen species and Caspase-3 activities.[52]

Table 2
CC_{50} values (μM) of **5a–f** obtained from the curves in Figure 5

Cell line	Triazole-containing alkyl xyloside surfactants							Control surfactants	
	5a	**5b**	**5c**	**5d**	**5e**	**5f**	**5g**	β-OXP	β-OTG
HaCaT	[a]	890 ± 50	120 ± 30	[a]	[a]	[a]	[a]	850 ± 30	490 ± 60
Hs27	[a]	694 ± 3	180 ± 50	[a]	[a]	[a]	[a]	760 ± 50	380 ± 30
Jurkat	[a]	580 ± 60	77 ± 9	26 ± 3	[a]	[a]	[a]	460 ± 13	310 ± 40

[a] Cytotoxicity was <50% at the highest compound concentration tested and therefore their CC_{50} values could not be determined. β-OXP: β-octyl xylopyranoside; β-OTG: β-octyl thioglucopyranoside.

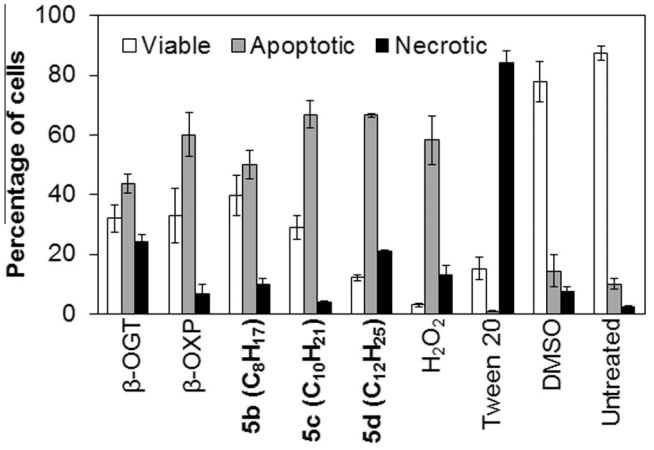

Figure 4. Percentage of viable, apoptotic, and necrotic Jurkat cells after 20 h of incubation, as determined by annexin V-FITC staining and flow cytometry. β-OGT (octyl β-thioglucopyranoside) and β-OXP (octyl β-xylopyranoside) were used for comparison. H_2O_2 (300 μM) was used as a positive control for apoptosis, and Tween 20 (0.5%) was used as a control for necrosis. Compounds were added at their CC_{50} value in DMSO. Error bars represent the standard deviation of the mean from three replicates. The chain length of the hydrophobic tail is indicated in parentheses.

2.4. Langmuir monolayer studies

The interfacial properties of surfactants are important for applications in pharmaceuticals, detergents, agrochemicals, and personal care products.[1] We characterized the ability of selected newly synthesized triazole-linked alkyl xylopyranosides to form monolayers at the air–water interface. Surface pressure isotherms were determined using a Langmuir balance at varying temperatures on a 150 mM NaCl/1.5 mM $CaCl_2$ subphase used previously to study monolayers under physiological conditions.[53,54] At 14 °C, only triazoles **5e** and **5f** formed stable monolayers. The compression isotherms of both compounds showed a single phase transition from an expanded to a condensed phase (Fig. 5). The phase transition displayed an 'overshoot' in surface pressure; the magnitude of the 'overshoot' does not appear to be temperature dependent. The 'overshoot' was greater for **5e** than **5f**, and likely indicates the initial formation of an unstable expanded monolayer, followed by slow reorganization to a stable monolayer in the condensed phase (Table 2). This phenomenon has been reported for different types of monolayers.[55–57] In all cases the kinetics of monolayer formation appear to be the driving force behind the unique shape of the compression isotherm. Further experiments are necessary to determine the nature of this phase transition of **5e** and **5f**.

The compression isotherms for **5e** and **5f** were recorded at different temperatures to verify that the breakpoints shown in Figure 5 are indeed attributable to a phase transition from an expanded to a condensed phase. For **5e** (containing a 14-carbon chain) the surface pressure at the phase transition, π_{trans}, increased from 5.6 mN/m at 14 °C to 26 mN/m at 30 °C (Fig. 4a and Table 3). The corresponding molecular area, A_{trans}, decreased from 68 Å^2/molecule to 38 Å^2/molecule in this temperature range. The same trends were observed for **5f**; the transition surface pressure, π_{trans}, increased from 1.6 to 18 mN/m, the transition area, A_{trans}, decreased from 83 to 51 Å^2/molecule, as the subphase temperature was increased from 17 to 37 °C. The changes in π_{trans} and A_{trans} as a function of temperature are shown in Figure 6. The dependence of phase transitions of insoluble monolayers at the air–water interface on temperature is well-known; comparable effects on expanded to condensed transitions have been shown for alkyl nicotinates,[58] partially fluorinated carboxylic acids,[59] and hydroxystearic acids.[60] When the plots of surface pressure at the phase transition

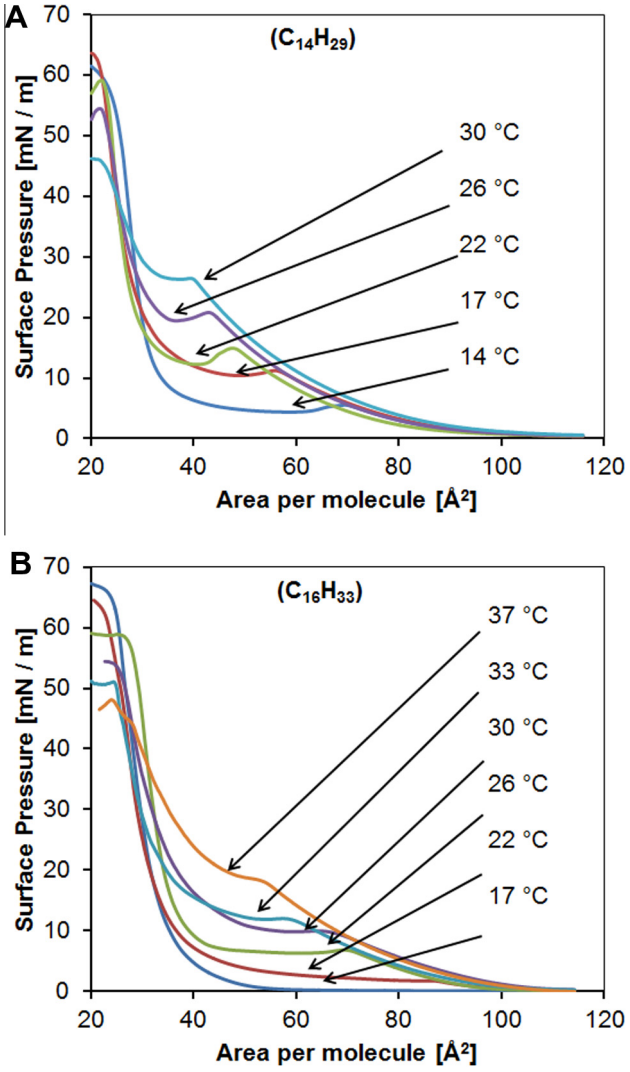

Figure 5. Representative compression isotherms (from three independent experiments) of (A) **5e** (tetradecyl chain) and (B) **5f** (hexadecyl side chain). The isotherms were obtained by symmetrical compression at 10 mm/min (7.5 cm^2/min) at the indicated temperature on a 150 mM NaCl/1.5 mM $CaCl_2$ subphase (pH = 7.0).

(π_{trans}) versus temperature (Fig. 6B) are extrapolated to zero surface pressure, the 'lift-off' temperature can be calculated;[61] this temperature corresponds to the point below which no phase transition occurs. For **5e** and **5f**, the values were 9.2 and 20.2 °C, respectively. Linear alkanoic acids follow the same trend: the 'lift-off' temperatures were approximately 7 °C for tetradecanoic acid (the saturated acid analog of **5e**) and 26 °C for hexadecanoic acid (the analog of **5f**).[61]

The limiting molecular areas, A_{lim}, of **5e** and **5f** were also dependent upon temperature. A_{lim} for **5e** increased from 31 Å^2/molecule at 14 °C to 42 Å^2/molecule at 30 °C, while A_{lim} for **5f** increased from 33 Å^2/molecule at 22 °C to 41 Å^2/molecule at 37 °C. At 26 °C, A_{lim} for **5e** and **5f** were 33 and 37 Å^2/molecule, respectively. A_{lim} did not show a strong temperature dependence, indicating that A_{lim} is primarily a function of the carbohydrate head group and/or the triazole linker. A_{lim} of saturated fatty acids are approximately 20 Å^2,[62] which reflects the cross-sectional area of hydrocarbon chains. For Gibbs monolayers of selected alkyl glucosides at the air–water interface, the limiting molecular area at 25 °C has been measured using the de Nouy method, with values of 42–44 Å^2/molecule for *n*-octyl, -decyl, and -dodecyl glucopyranosides.[63] At 25 °C, the

Table 3
Temperature-dependence of parameters determined from the isotherms presented in Figure 5 for **5e** (tetradecyl chain) and **5f** (hexadecyl chain)

Compound	Temperature (°C)	π_{trans}	A_{trans}	A_{lim}	π_{max}	C_{max}
5e	14	5.6 ± 0.2	68.5 ± 0.9	31. ± 2.0	64.1 ± 0.5	250 ± 20
	17	11.3 ± 0.2	53.6 ± 0.9	29.6 ± 0.6	62.4 ± 1.4	200 ± 20
	22	15.0 ± 0.1	47.5 ± 0.2	29.7 ± 0.7	59.4 ± 0.6	233 ± 1
	26	20.9 ± 0.2	42.1 ± 0.7	32.8 ± 1.2	53.0 ± 2.0	140 ± 2
	30	27.0 ± 0.5	38.0 ± 1.2	41.6 ± 0.4	47.0 ± 3.0	71 ± 3
5f	22	1.6 ± 0.2	84.0 ± 2.0	32.9 ± 1.1	64.0 ± 3.0	250 ± 50
	26	6.8 ± 0.1	70.0 ± 2.0	37.0 ± 2.0	58.6 ± 0.8	239 ± 20
	30	9.9 ± 0.1	65.0 ± 2.0	41.0 ± 5.0	53.6 ± 1.0	146 ± 5
	33	11.6 ± 0.3	61.0 ± 2.0	41.0 ± 3.0	51.6 ± 0.4	130 ± 20
	37	18.4 ± 0.4	51.2 ± 0.9	41.8 ± 0.2	48.0 ± 2.0	102 ± 11

T: temperature of the subphase; A_{lim}: limiting molecular area (Å^2/molecule); A_{trans}: mean molecular area at phase transition (Å^2/molecule); π_{trans}: surface pressure at phase transition (mN/m); π_{max}: maximum surface pressure (mN/m); C_{max}: maximum compressibility.

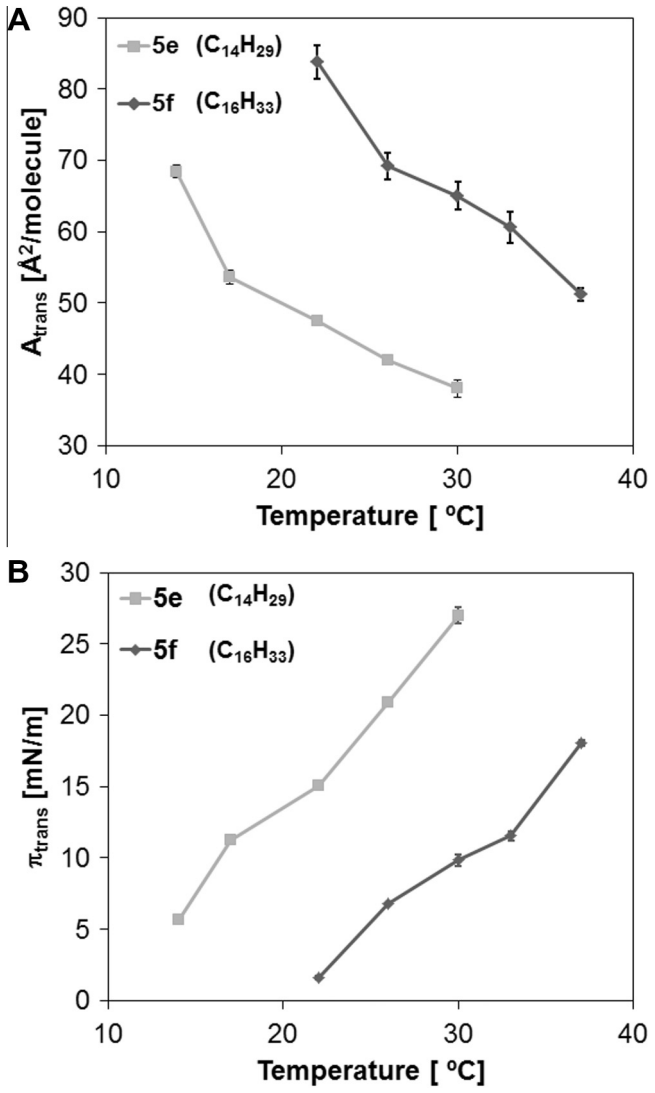

Figure 6. Temperature dependence of (A) average molecular area, A_{trans}, and (B) surface pressure, π_{trans}, at the phase transition for **5e** (tetradecyl chain) and **5f** (hexadecyl chain). The values presented are the average of at least three experiments, with standard deviation.

limiting molecular areas of n-octyl glucosamine and *n*-nonyl glucosamine were 48 and 46 Å^2/molecule, respectively.[64] These literature values are consistent with in silico calculations.[20] 6-*O*-Stearoyl hexoses formed insoluble monolayers at the air–water interface with limiting molecular areas of 44 Å^2 for 6-*O*-stearoyl glucopyranoside and 32 Å^2 for 6-*O*-stearoyl galactopyranoside.[65] These values are comparable to the limiting molecular areas for the triazole-linked surfactants **5e** and **5f** reported here. This observation suggests that the cross-sectional area of the carbohydrate moiety may determine the limiting molecular area of **5e** and **5f**.

The collapse pressure, π_{max}, also decreased with increasing temperature, ranging from 64 to 47 mN/m for both **5e** and **5f**, as expected for stable surfactant monolayers. This follows the trend seen in DPPC monolayers as a function of temperature.[66] The collapse pressures for 6-*O*-stearoyl glucopyranoside and 6-*O*-stearoyl galactopyranoside were 43 and 66 mN/m, respectively, at room temperature,[65] which is comparable to the collapse pressures of **5e** and **5f**. The compressibility modulus was obtained from the compression isotherms using the equation $C_s = -A\ (\delta\Pi/\delta A)$; the graphs of compressibility versus surface pressure exhibited a temperature-dependent peak. The maximum compressibility, C_{max}, ranged from 251 to 71 mN/m for **5e** and 247 to 102 mN/m for **5f**, and decreased with increasing temperature. This property of surfactants has been discussed in the literature, although not for carbohydrate-based surfactants;[67] the effect is likely due to an increase in fluidity of the monolayer.

2.5. Conclusions

In this paper we reported the synthesis and characterization of novel alkyl xylopyranosides, incorporating a 1,2,3-triazole linker. The compounds were synthesized using 'click chemistry' in moderate to excellent yields. Unlike previously reported alkyl xylopyranosides[8] and glucose-based triazole-containing surfactants,[15] the triazole-linked surfactants **5a**–**g** did not exhibit liquid–crystalline properties, as assessed using DSC. Further studies of their liquid–crystalline properties are therefore warranted. The compounds did exhibit other properties of surfactants (i.e., they formed stable monolayers at the air–water interface). The potential biocompatibility of the surfactants was tested, as they have potential uses in various consumer applications. The triazole-linked surfactants with short or long chains were shown to be non-toxic in several mammalian cell lines. Intermediate length surfactants exhibited low cytotoxicity, primarily through apoptosis, with CC values in the high micromolar range. Overall, triazole-linked surfactants merit further investigation because they are readily synthesized from renewable starting materials, and display low toxicity and surface activity.

3. Experimental procedures

3.1. General methods

The ^{1}H and ^{13}C NMR spectra were recorded on multinuclear Bruker Avance 300 or Bruker DRX 400 Digital NMR spectrometers.

Spectral assignments were determined from COSY experiments. ^{19}F spectra were recorded using a Bruker Avance 300. The mass spectra were measured at the University of California, Riverside Mass Spectrometry facility. Elemental analyses were obtained from Atlantic Micro Lab Microanalysis Service (Atlanta, Georgia, USA). Melting points were determined using a MelTemp apparatus, and are uncorrected. All reactions were monitored by thin layer chromatography, followed by visualization with UV and anisaldehyde–H_2SO_4. 1,2,3,4-Tetra-*O*-acetyl-β-D-xylose (**2**)[21] and propargyl 2,3,4-tri-*O*-acetyl-β-D-xylopyranoside (**3**)[23] were prepared as described previously. Azides were synthesized using a known method[24] and used without further purification. Propargyl alcohol and Dowex® 50 W × 8–100 ion exchange resin were obtained from Acros. Sodium methoxide was obtained from Alfa Aesar. Sodium azide and sodium ascorbate were obtained from Sigma–Aldrich. Cupric sulfate pentahydrate was obtained from Mallinckrodt. All organic solvents were reagent grade or higher, and used without further purification. Flash chromatography was performed using 60 Å (40–63 μm, 230 × 400 mesh) silica gel with the indicated solvent mixture.

3.2. General procedure for the CuAAC reaction

Triacetyl propargyl xylose **3** and n-alkyl azide (1.0–1.1 equiv) were combined with 2:1 tBuOH/water (0.33 M) at room temperature. Sodium ascorbate (0.2 equiv, 1.0 M in water) was added, followed by $CuSO_4$ pentahydrate (0.1 equiv, 75 mg/mL in water), and the mixture was stirred at room temperature for 90 min. At this time the reactions often became homogeneous and faint blue. The reaction mixture was diluted with water and extracted three times with ethyl acetate. The combined extracts were washed with brine, dried over $MgSO_4$, and concentrated. The crude residue was purified by silica gel column chromatography (hexanes/EtOAc).

3.2.1. (1-Hexyl-1*H*-1,2,3-triazol-4-yl)methyl 2,3,4-tri-*O*-acetyl-β-xylopyranoside (4a)

Following the general procedure with propargyl xylose **3** (427 mg, 1.35 mmol) and *n*-hexyl azide (172 mg, 1.35 mmol), then column chromatography using EtOAc/hexanes (1:1, v/v), 462 mg (78%) of **4a** was obtained as a clear oil, which solidified upon standing. ^1H NMR (400 MHz, $CDCl_3$): δ 7.49 (s, 1H, triazole-CH), 5.16 (pseudo t, J ~8.5 Hz, 1H, H-3), 4.89–4.99 (m, 3 H, H-1′a, H-2, H-4), 4.78 (d, J = 12.5 Hz, 1H, H-1′b), 4.64 (d, J = 6.8 Hz, 1H, H-1), 4.34 (t, J = 7.3 Hz, 2H, triazole-N-CH_2), 4.14 (dd, J = 11.8, 5.1 Hz, 1H, H-5e), 3.40 (dd, J = 11.8, 8.8 Hz, 1 H, H-5a), 2.05 (s, 3H, OCOCH_3), 2.02 (s, 3 H, OCOCH_3), 2.00 (s, 3H, OCOCH_3), 1.83–1.95 (m, 2H, triazole-N-CH_2CH_2), 1.25–1.36 (m, 6H, 3 × CH_2), 0.88 (t, J = 6.9 Hz, 3H, RCH_3); ^{13}C NMR (100 MHz, $CDCl_3$): δ 170.0, 169.8, 169.4, 144.2, 122.3, 100.0, 71.4, 70.8, 68.8, 62.6, 62.1, 50.4, 31.1, 30.2, 26.1, 22.3, 20.67, 20.63 (2 × C), 13.9; HRESIMS calcd for $C_{20}H_{32}N_3O_8$ $(M+H)^+$: 442.2184; found: 442.2184; Anal. calcd for $C_{20}H_{31}N_3O_8$: C 54.41; H 7.08; N 9.52; found: C 54.49; H 7.09; N 9.54.

3.2.2. (1-Octyl-1*H*-1,2,3-triazol-4-yl)methyl 2,3,4-tri-O-acetyl-β-xylopyranoside (4b)

Following the general procedure with propargyl xylose **3** (462 mg, 1.47 mmol) and *n*-octyl azide (259 mg, 1.66 mmol), then column chromatography using EtOAc:hexanes (1:1, v/v), 511 mg (74%) of **4b** was obtained as a clear oil which, solidified upon standing. ^1H NMR (400 MHz, $CDCl_3$): δ 7.48 (s, 1H, triazole-CH), 5.15 (pseudo t, J ~8.7 Hz, 1H, H-3), 4.84–5.02 (m, 3H, H-1′a, H-2, H-4), 4.77 (d, J = 12.6 Hz, 1H, H-1′b), 4.63 (d, J = 6.8 Hz, 1H, H-1), 4.33 (t, J = 7.3 Hz, 2H, triazole-NCH_2), 4.13 (dd, J = 11.9, 5.1 Hz, 1H, H-5e), 3.39 (dd, J = 11.9, 8.8 Hz, 1H, H-5a), 2.04 (s, 3H OCOCH_3), 2.01 (s, 3H OCOCH_3), 1.99 (s, 3H OCOCH_3), 1.82–1.93 (m, 2H, triazole-N-CH_2CH_2), 1.17–1.37 (m, 10H, 5 × CH_2), 0.86 (t, J = 6.7 Hz, 3H RCH_3); ^{13}C NMR (100 MHz, $CDCl_3$): δ 170.0, 169.8, 169.4, 144.1, 122.3, 99.8, 71.3, 70.7, 68.7, 62.5, 62.0, 50.3, 31.6, 30.2, 29.0, 28.9, 26.4, 22.5, 20.70, 20.66 (2 × C), 14.0; HRESIMS calcd for $C_{22}H_{36}N_3O_8$ $(M+H)^+$: 470.2497; found: 470.2505; Anal calcd for $C_{22}H_{35}N_3O_8$: C 56.28; H 7.51; N 8.95; found: C 56.63; H 7.48; N 8.97.

3.2.3. (1-Decyl-1*H*-1,2,3-triazol-4-yl)methyl 2,3,4-tri-O-acetyl-β-xylopyranoside (4c)

Following the general procedure with propargyl xylose **3** (438 mg, 1.39 mmol) and *n*-decyl azide (263 mg, 1.43 mmol), then column chromatography using EtOAc:hexanes (2:1, v/v), 407 mg (74%) of **4c** was obtained as a clear oil which, solidified upon standing. ^1H NMR (400 MHz, $CDCl_3$): δ 7.50 (s, 1H, triazole-CH), 5.17 (pseudo t, J ~8.4 Hz, 1H, H-3), 4.87–5.00 (m, 3H, H-1′a, H-2, H-4), 4.78 (d, J = 12.6 Hz, 1H, H-1′b), 4.64 (d, J = 6.9 Hz, 1H, H-1), 4.34 (t, J = 7.3 Hz, 2H, triazole-NCH_2), 4.15 (dd, J = 11.9, 5.1 Hz, 1H, H-5e), 3.40 (dd, J = 11.9, 8.8 Hz, 1H, H-5a), 2.06 (s, 3H, OCOCH_3), 2.03 (s, 3H, OCOCH_3), 2.02 (s, 3H, OCOCH_3), 1.83–1.96 (m, 2H, triazole-N-CH_2CH_2), 1.14–1.40 (m, 14H, 7 × CH_2), 0.88 (t, J = 6.7 Hz, 3H RCH_3); ^{13}C NMR (100 MHz, $CDCl_3$): δ 170.0, 169.9, 169.5, 144.1, 122.4, 99.8, 71.3, 70.7, 68.8, 62.6, 62.1, 50.4, 31.8, 30.3, 29.4, 29.3, 29.2, 29.0, 26.4, 22.6, 20.75, 20.70 (2 × C), 14.1; HRESIMS m/z calcd for $C_{24}H_{40}N_3O_8$ $(M+H)^+$: 498.2810; found: 498.2824; Anal. calcd for $C_{24}H_{39}N_3O_8$: C 57.93; H 7.90; N 8.44; found: C 57.92; H 7.86; N 8.45.

3.2.4. (1-Dodecyl-1*H*-1,2,3-triazol-4-yl)methyl 2,3,4-tri-O-acetyl-β-xylopyranoside (4d)

Following the general procedure with propargyl xylose **3** (431 mg, 1.37 mmol) and *n*-dodecyl azide (297 mg, 1.40 mmol) then column chromatography using EtOAc:hexanes (3:2, v/v), 463 mg (64%) of **4d** was obtained as a waxy white solid. ^1H NMR (400 MHz, $CDCl_3$): δ 7.48 (s, 1H, triazole-CH), 5.15 (pseudo t, J ~8.5 Hz, 1H, H-3), 4.87–4.98 (m, 3H, H-1′a, H-2, H-4), 4.77 (d, J = 12.4 Hz, 1H, H-1′b), 4.64 (d, J = 6.8 Hz, 1H, H-1), 4.33 (t, J = 7.2 Hz, 2H, triazole-NCH_2), 4.14 (dd, J = 11.8, 5.2 Hz, 1H, H-5e), 3.40 (dd, J = 11.8, 8.8 Hz, 1H, H-5a), 2.04 (s, 3H, OCOCH_3), 2.01 (s, 3H, OCOCH_3), 2.00 (s, 3H, OCOCH_3), 1.82–1.94 (m, 2H, triazole-N-CH_2CH_2), 1.15–1.39 (m, 18H, 9 × CH_2), 0.87 (t, J = 6.6 Hz, 3H RCH_3); ^{13}C NMR ($CDCl_3$,100 MHz): δ 170.0, 169.8, 169.4, 144.1, 122.3, 99.8, 71.4, 70.8, 68.8, 62.6, 62.1, 50.4, 31.8, 30.3, 29.54 (2 × C), 29.46, 29.33, 29.27, 28.9, 26.4, 22.6, 20.68, 20.64 (2 × C), 14.1; HRESIMS calcd for $C_{26}H_{44}N_3O_8$ $(M+H)^+$: 526.3123; found: 526.3134; Anal. calcd for $C_{26}H_{43}N_3O_8$: C 59.41; H 8.25; N 7.99; found: C 59.67; H 8.14; N 7.96.

3.2.5. (1-Tetradecyl-1*H*-1,2,3-triazol-4-yl)methyl 2,3,4-tri-O-acetyl-β-D-xylopyranoside (4e)

Following the general procedure with propargyl xylose **3** (419 mg, 1.33 mmol) and n-tetradecyl azide (355 mg, 1.48 mmol), then column chromatography using EtOAc:hexanes (2:1, v/v), 537 mg (73%) of **4e** was obtained as a waxy white solid. ^1H NMR (400 MHz, $CDCl_3$): δ 7.49 (s, 1H, triazole-CH), 5.16 (pseudo t, J ~8.2 Hz, 1H, H-3), 4.88–5.00 (m, 3H, H-1′a, H-2, H-4), 4.78 (d, J = 12.5 Hz, 1H, H-1′b), 4.65 (d, J = 6.9 Hz, 1H, H-1), 4.33 (t, J = 7.3 Hz, 2H, triazole-NCH_2), 4.15 (dd, J = 11.9, 5.1 Hz, 1H, H-5e), 3.40 (dd, J = 11.9, 8.8 Hz, 1H, H-5a), 2.05 (s, 3H, OCOCH_3), 2.02 (s, 3H, OCOCH_3), 2.01 (s, 3H, OCOCH_3), 1.82–1.95 (m, 2H, triazole-N-CH_2CH_2), 1.18–1.39 (m, 22H, 11 × CH_2), 0.88 (t, J = 6.6 Hz, 3H RCH_3); ^{13}C NMR ($CDCl_3$,100 MHz): δ 170.0, 169.9, 169.4, 144.2, 122.3, 99.9, 71.4, 70.8, 68.9, 62.6, 62.1, 50.4, 31.9, 30.3, 29.65, 29.61 (2 × C), 29.57, 29.5, 29.4, 29.3, 29.0, 26.5, 22.7, 20.72, 20.68 (2 × C), 14.1; HRESIMS calcd for $C_{28}H_{48}N_3O_8$ $(M+H)^+$: 554.3436;

found: 554.3442; Anal. calcd for $C_{28}H_{47}N_3O_8$: C 60.74; H 8.56; N 7.59; found C 60.46; H 8.57; N 7.65.

3.2.6. (1-Hexadecyl-1*H*-1,2,3-triazol-4-yl)methyl 2,3,4-tri-*O*-acetyl-β-D-xylopyranoside (4f)

Following the general procedure with propargyl xylose **3** (420 mg, 1.34 mmol) and n-hexadecyl azide (369 mg, 1.38 mmol), then column chromatography using EtOAc:hexanes (2:1, v/v), 621 mg (80%) of **4e** was obtained as a waxy white solid. ^{1}H NMR ($CDCl_3$,400 MHz): δ 7.48 (s, 1H, triazole-CH), 5.15 (pseudo t, J ~8.8 Hz, 1H, H-3), 4.86–4.98 (m, 3H, H-1′a, H-2, H-4), 4.76 (d, J = 11.5 Hz, 1H, H-1′b), 4.63 (d, J = 6.8 Hz, 1H, H-1), 4.32 (J = 7.2 Hz, 2H, triazole-NCH_2), 4.13 (dd, J = 11.9, 5.1 Hz, 1H, H-5e), 3.39 (dd, J = 11.9, 8.8 Hz, 1H, H-5a), 2.04 (s, 3H, OCOCH_3), 2.01 (s, 3H, OCOCH_3), 2.00 (s, 3H, OCOCH_3), 1.83–1.94 (m, 2H, triazole-N-CH_2CH_2), 1.17–1.37 (m, 26H, 13 × CH_2), 0.87 (t, J = 6.6 Hz, 3H RCH_3); ^{13}C NMR ($CDCl_3$,100 MHz): δ 169.9, 169.8, 169.4, 144.1, 122.3, 99.8, 71.3, 70.7, 68.8, 62.5, 62.1, 50.3, 31.9, 30.2, 29.62, 29.61 (2 × C), 29.58 (2 × C), 29.53, 29.46, 29.32, 29.28, 28.9, 26.4, 22.6, 20.66, 20.63 (2 × C), 14.0; HRESIMS calcd for $C_{30}H_{52}N_3O_8$ $(M+H)^+$: 582.3749; found: 582.3761; Anal. Calcd for $C_{30}H_{51}N_3O_8$: C 61.94; H 8.84; N 7.22; found: C 61.66; H 8.91; N 6.96.

3.2.7. (1-(3,3,4,4,5,5,6,6,7,7,8,8,8-Tridecafluorooctyl)-1*H*-1,2,3-triazol-4-yl)methyl 2,3,4-tri-O-acetyl-β-D-xylopyranoside (4g)

Following the general procedure with propargyl[68] xylose **3** (430 mg, 1.27 mmol) and 3,3,4,4,5,5,6,6,7,7,8,8,8-tridecafluorooctyl azide (550mg, 1.41 mmol), then column chromatography using EtOAc:hexanes (2:1, v/v), 743 mg (77%) of a waxy white solid was obtained. ^{1}H NMR ($CDCl_3$,400 MHz): δ (ppm): 7.58 (s, 1H, triazole-CH), 5.17 (pseudo t, J ~8.5 Hz, 1H, H-3), 4.90–5.01 (m, 3H, H-1′a, H-2, H-4), 4.79 (d, J = 13.1 Hz, 1H, H-1′b), 4.68 (t, J = 7.2 Hz, 2H, triazole-NCH_2), 4.64 (d, J = 6.6 Hz, 1H, H-1), 4.16 (dd, J = 11.9, 5.1 Hz, 1H, H-5e), 3.41 (dd, J = 11.9, 8.7 Hz, 1H, H-5a), 2.84 (tt, J = 17.9, 7.5 Hz, 2H, triazole-N-CH_2CH_2), 2.05 (s, 3H, OCOCH_3), 2.03 (s, 3H, OCOCH_3), 2.01 (s, 3H, OCOCH_3); ^{13}C NMR (100 MHz, $CDCl_3$): δ 170.0, 169.9, 169.5, 144.8, 123.1, 99.9, 71.3, 70.8, 68.8, 62.4, 62.1, 42.5, 31.7, 20.70, 20.65, 20.62; ^{19}F NMR (282 MHz, $CDCl_3$): δ −81.3, −114.6, −122.3, −123.3, −123.9, −126.6; HRESIMS calcd for $C_{22}H_{23}$ $F_{13}N_3O_8$ $(M+H)^+$: 704.1272; found: 704.1297; Anal. Calcd for $C_{22}H_{22}F_{13}N_3O_8$: C 37.57; H 3.15; N 5.97; found: C 37.56; H 3.01; N 5.91.

3.3. General procedure for acetate removal[8]

Triazole peracetates **4** were stirred in dry methanol. NaOMe (3–4 equiv) was added and the solution stirred at room temperature for two hours. Dowex® 50 W × 8–100 ion exchange resin was added and the reaction mixture stirred for another 30 min. The resin was filtered and the solvent concentrated. The crude residue was purified by recrystallization to yield pure 1-alkyl-1*H*-1,2,3-triazol-4-yl)methyl β-D-xylopyranosides **5**.

3.3.1. (1-Hexyl-1*H*-1,2,3-triazol-4-yl)methyl β-D-xylopyranoside (5a)

Triazole **4a** (443 mg, 1.00 mmol) was deprotected using the general conditions and purified by recrystallization from chloroform to yield 160 mg (51%) of a white solid. ^{1}H NMR (CD_3OD,400 MHz): δ 7.98 (s, 1H, triazole-CH), 4.90 (d, J = 12.4 Hz, 1H, H-1′a), 4.73 (d, J = 12.4 Hz, 1H, H-1′b), 4.39 (t, J = 7.1 Hz, 2H, triazole-NCH_2), 4.32 (d, J = 7.5 Hz, 1H, H-1), 3.88 (dd, J = 11.4, 5.3 Hz, 1H, H-5e), 3.49 (m, 1H, H-4), 3.28–3.34 (m, 1H, overlapping with CD_3OD peak, H-5a), 3.17–3.26 (m, 2H, H-2, H-3), 1.88–1.93 (m, 2H, triazole-N-CH_2CH_2), 1.21–1.43 (m, 6H, 3 × CH_2), 0.90 (t, J = 6.9 Hz, 3H, CH_3); ^{13}C NMR (100 MHz, CD_3OD): δ 145.8, 125.2, 104.4, 77.9, 75.0, 71.3, 67.2, 63.2, 51.5, 32.4, 31.4, 27.3, 23.6, 14.4; HRESIMS calcd for $C_{14}H_{26}N_3O_5$ $(M+H)^+$: 316.1867; found: 316.1873; Anal calcd for $C_{14}H_{25}N_3O_5$: C 53.32; H 7.99; N 13.32; found: C 53.08; H 7.97; N 13.17.

3.3.2. (1-Octyl-1*H*-1,2,3-triazol-4-yl)methyl β-D-xylopyranoside (5b)

Triazole **4b** (441 mg, 0.939 mmol) was deprotected using the general conditions and purified by recrystallization from ethanol-hexanes to yield 160 mg (50%) of a white solid. ^{1}H NMR (400 MHz, CD_3OD): δ 7.97 (s, 1H, triazole-CH), 4.91 (d, J = 12.3 Hz, 1H, H-1′a), 4.73 (d, J = 12.3 Hz, 1H, H-1′b), 4.39 (t, J = 7.1 Hz, 2H, triazole-NCH_2), 4.32 (d, J = 7.5 Hz, 1H, H-1), 3.88 (dd, J = 11.4, 5.3 Hz, 1H, H-5e), 3.49 (m, 1H, H-4), 3.28–3.34 (m, 1H, overlapping with CD_3OD, H-5a), 3.16–3.26 (m, 2H, H-2, H-3), 1.79–1.97 (m, 2H, triazole-N-CH_2CH_2), 1.20–1.39 (m, 10H, 5 × CH_2), 0.89 (t, J = 6.6 Hz, 3H, CH_3); ^{13}C NMR (100 MHz, CD_3OD): δ 145.6, 125.1, 104.3, 77.8, 74.9, 71.2, 67.0, 63.0, 51.4, 32.9, 31.3, 30.2, 30.0, 27.5, 23.7, 14.4; HRESIMS calcd for $C_{16}H_{30}N_3O_5$ $(M+H)^+$: 344.2180; found: 344.2179; Anal. calcd for $C_{16}H_{29}N_3O_5$: C 55.96; H 8.51; N 12.24; found: C 55.82; H 8.51; N 12.21.

3.3.3. (1-Decyl-1*H*-1,2,3-triazol-4-yl)methyl β-D-xylopyranoside (5c)

Triazole **4c** (400 mg, 0.804 mmol) was deprotected using the general conditions and purified by recrystallization from acetone to yield 163 mg (55%) of a white solid. ^{1}H NMR (400 MHz, CD_3OD): δ 7.97 (s, 1H, triazole-CH), 4.90 (d, J = 12.3 Hz, 1H, H-1′a), 4.73 (d, J = 12.3 Hz, 1H, H-1′b), 4.39 (t, J = 7.1 Hz, 2H, triazole-NCH_2), 4.32 (d, J = 7.5 Hz, 1H, H-1), 3.88 (dd, J = 11.4, 5.4 Hz, 1H, H-5e), 3.49 (m, 1H, H-4), 3.27–3.36 (m, 1H, overlapping with CD_3OD, H-5a), 3.15–3.27 (m, 2H, H-2, H-3), 1.81–2.01 (m, 2H, triazole-N-CH_2CH_2), 1.14–1.42 (m, 14H, 7 × CH_2), 0.90 (t, J = 6.7 Hz, 3H, CH_3); ^{13}C NMR (100 MHz, CD_3OD): δ 145.6, 125.1, 104.3, 77.8, 74.9, 71.2, 67.0, 63.0, 51.4, 33.0, 31.3, 30.6, 30.5, 30.4, 30.1, 27.4, 23.7, 14.4; HRESIMS calcd for $C_{18}H_{34}N_3O_5$ $(M+H)^+$: 372.2504; found: 372.2499; Anal. calcd for $C_{18}H_{33}N_3O_5$: C 58.18; H 8.96; N 11.32; found: C 58.17; 8.92; N 11.28.

3.3.4. (1-Dodecyl-1*H*-1,2,3-triazol-4-yl)methyl β-D-xylopyranoside (5d)

Triazole **4d** (566 mg, 1.08 mmol) was deprotected using the general conditions and purified by recrystallization from acetone to yield 278 mg (65%) of a white solid. ^{1}H NMR (400 MHz, DMSO-d_6): δ 8.07 (s, 1H, triazole-CH), 5.03 (d, J = 5.0 Hz, 1H, OH), 4.95 (pseudo d, J = 2.7 Hz, 2H, 2 × OH), 4.76 (d, J = 12.1 Hz, 1H, H-1′a), 4.58 (d, J = 11.3 Hz, 1H, H-1′b), 4.32 (t, J = 7.1 Hz, 2H, triazole-NCH_2), 4.22 (d, J = 7.5 Hz, 1H, H-1), 3.73 (dd, J = 11.3, 5.3 Hz, 1H, H-5e), 3.23–3.30 (m, 1H, H-4), 2.91–3.14 (m, 3H, H-2, H-3, H-5a), 1.71–1.85 (m, 2H, triazole-N-CH_2CH_2), 1.11–1.35 (m, 9 × CH_2), 0.85 (t, J = 6.7 Hz, 3H); ^{13}C NMR (100 MHz, DMSO-d_6): δ 143.6, 123.9, 102.8, 76.6, 73.2, 69.6, 65.7, 61.5, 49.3, 31.3, 29.7, 29.0 (2 × C), 28.95, 28.86, 28.7, 28.4, 25.8, 22.1, 13.9; HRESIMS calcd for $C_{20}H_{38}N_3O_5$ $(M+H)^+$: 400.2806; found: 400.2806; Anal calcd for $C_{20}H_{37}N_3O_5$: C 60.11; H 9.34; N 10.52; found: C 60.08; H 9.41; N 10.49.

3.3.5. (1-Tetradecyl-1*H*-1,2,3-triazol-4-yl)methyl β-D-xylopyranoside (5e)

Triazole **4e** (435 mg, 0.786 mmol) was deprotected using the general conditions and purified by recrystallization from acetone to yield 218 mg (65%) of a white solid. ^{1}H NMR (400 MHz, DMSO-d_6): δ 8.07 (s, 1H, triazole-CH), 5.01–5.07 (br s, 1H, OH), 4.94–5.00 (m, 2H, 2 × OH), 4.76 (d, J = 12.1 Hz, 1H, H-1′a), 4.58 (d, J = 12.1 Hz, 1H, H-1′b), 4.32 (t, J = 7.1 Hz, 2H, triazole-NCH_2), 4.22 (d, J = 7.6 Hz, 1H, H-1), 3.73 (dd, J = 11.3, 5.3 Hz, 1H, H-5e),

3.20–3.33 (m, 1H, H-4), 2.96–3.12 (m, 3H, H-2, H-3, H-5a), 1.66–1.91 (m, 2H, triazole-N-CH_2CH_2), 1.06–1.40 (m, 11 × CH_2), 0.85 (t, J = 6.6 Hz, 3H, CH_3); ^{13}C NMR (100 MHz, DMSO-d_6): δ 143.6, 123.9, 102.8, 76.6, 73.2, 69.6, 65.8, 61.5, 49.3, 31.3, 29.7, 29.0, 29.0 (2 × C), 29.0, 28.9, 28.9, 28.7, 28.4, 25.8, 22.1, 13.9; HRESIMS calcd for $C_{22}H_{42}N_3O_5$ $(M+H)^+$: 428.3119; found: 428.3118; Anal. calcd for $C_{22}H_{41}N_3O_5$: C 61.78; H 9.57; N 9.83; found: C 61.52; H 9.41; N 9.69.

3.3.6. (1-Hexadecyl-1*H*-1,2,3-triazol-4-yl)methyl β-D-xylopyranoside (5f)

Triazole **5f** (447 mg, 0.763 mmol) was deprotected using the general conditions and purified by recrystallization from chloroform to yield 259 mg (74%) of a white solid. ^{1}H NMR (400 MHz, DMSO-d_6): δ 8.07 (s, 1H, triazole-CH), 5.03 (d, J = 5.1 Hz, 1H, OH), 4.95 (dd, J = 4.8, 3.1 Hz, 2H, 2 × OH), 4.76 (d, J = 12.2 Hz, 1H, H-1′a), 4.58 (d, J = 12.0 Hz, 1H, H-1′b), 4.32 (t, J = 7.1, 2H, triazole-NCH_2), 4.22 (d, J = 7.6 Hz, 1H, H-1), 3.73 (dd, J = 11.2, 5.4 Hz, 1H, H-5e), 3.21–3.32 (m, 1H, H-4), 2.91–3.15 (m, 3H, H-2, H-3, H-5a), 1.68–1.88 (m, 2H, triazole-N-CH_2CH_2), 1.08–1.34 (m, 13 × CH_2), 0.85 (t, J = 6.6 Hz, 3H, CH_3); ^{13}C NMR (100 MHz, DMSO-d_6): δ = 143.6, 123.9, 102.8, 76.5, 73.2, 69.6, 65.7, 61.5, 49.3, 31.3, 29.7, 29.0 (4 × C), 29.0 (2 × C), 28.9, 28.9, 28.7, 28.4, 25.8, 22.1, 13.9; HRESIMS calcd for $C_{24}H_{46}N_3O_5$ $(M+H)^+$: 456.3432; found: 456.3434; Anal. calcd for $C_{24}H_{45}N_3O_5$: C 63.25; H 9.96; N 9.23; found: C 63.01; H 9.83; N 9.12.

3.3.7. (1-(3,3,4,4,5,5,6,6,7,7,8,8,8-Tridecafluorooctyl)-1*H*-1,2,3-triazol-4-yl)methyl β-D-xylopyranoside (5g)

Triazole **4g** (400, mg, 0.597 mmol) was deprotected using the general conditions and purified by recrystallization from chloroform to yield 192 mg (56%) of a white solid. ^{1}H NMR (400 MHz, DMSO-d_6): δ 8.21 (s, 1H, triazole-CH), 5.02 (d, J = 5.1 Hz, 5H, OH), 4.95 (d, J = 4.9 Hz, 2H, 2 × OH), 4.78 (d, J = 12.2 Hz, 1H, H-1′a), 4.72 (t, J = 7.0 Hz, 2H, triazole-NCH_2), 4.60 (d, J = 11.3 Hz, 1H, H-1′b), 4.23 (d, J = 7.6 Hz, 1H, H-1), 3.73 (dd, J = 11.3, 5.3 Hz, 1H, H-5e), 3.25–3.31 (m, 1H, H-4), 2.97–3.09 (m, 5H, H-2, H-3, H-5a, triazole-N-CH_2CH_2); ^{13}C NMR (100 MHz, DMSO-d_6): δ 143.8, 124.5, 102.8, 76.6, 73.2, 69.5, 65.7, 61.3, 41.6, 30.3; ^{19}F NMR (282 MHz, DMSO-d_6): δ −79.76, −113.02, −121.26, −122.17, −122.66, −125.29. HRESIMS calcd for $C_{16}H_{17}F_{13}N_3O_5$ $(M+H)^+$: 578.0955; found: 578.0969; Anal. calcd for $C_{16}H_{16}F_{13}N_3O_5$ $(M+H)^+$: C 33.29; H 2.79; N 7.28; found: C 33.51; H 2.62; N 7.16.

3.4. Differential scanning calorimetry

Before starting the DSC experiments the TA Instruments Q200 instrument (TA Instruments, New Castle, DE) was calibrated with indium for temperature and enthalpy accuracy. Samples were prepared by weighing 1.0–1.5 mg of the dry surfactant into pre-weighed Tzero aluminum pans. Tzero hermetic lids were then pressed onto the pan. Empty Tzero pans with Tzero hermetic lid were used as the reference sample. The thermal analysis was performed between 25 and 200 °C with a ramp rate of 2.5 °C/min. The phase transitions were analyzed using Universal Analysis software (TA Instruments).

3.5. Cell culture experiments

3.5.1. Stock solutions

All compounds were dissolved in DMSO at 100 μM. Solubility under experimental conditions was verified by adding 2 μL of each solution to 200 μL of cell culture medium, vortexed for 5 s, centrifuged at 1,400 rpm (357×g) for 1 min before inspection for precipitation.

3.5.2. Cell lines and cell culture

Spontaneously immortalized human keratinocytes (HaCaT), normal non-transformed human foreskin fibroblasts (Hs27) and human acute leukemia T lymphocytes (Jurkat) were used to evaluate the cytotoxicity of **5a–g**. HaCaT and Hs27 cells were maintained in Dubelcco's Modified Eagle Medium (DMEM; HyClone, Logan, UT) with 10% heat-inactivated newborn calf serum (NCS; HyClone). Jurkat cells were maintained in RPMI media with 10% heat-inactivated FBS (HyClone). Penicillin (100 U/mL), streptomycin (100 μg/mL) and amphotericin B (0.25 μg/mL) were added to the media to prevent microbial contamination. Cells were incubated at 37 °C with 5% CO_2.

3.5.3. MTS assay

Cells were seeded in flat bottom MICROTEST™ tissue culture 96-well plates (Becton Dickinson Labware, Franklin Lakes, NJ) at a density of 5000 (HaCaT and Hs27 cells) or 25,000 (Jurkat cells). Compounds **5a–g** in DMSO were added to the cells at concentrations of 1–1000 μM. After 18 h (HaCaT and Hs27 cells) or 16 h (Jurkat cells), MTS (20 μL, CellTiter 96 AQ_{ueous}One Solution Cell Proliferation Assay; Promega, Madison, WI) was added to each well. The cells were further incubated for 2 h (HaCaTand Hs27 cells) or 4 h (Jurkat cells). The absorbance of formazan at 490 nm was measured using a microplate reader ($VERSA_{max}$ tunable microplate reader, MDS, Inc., Toronto, Canada). Absorbance at 650 nm was used as a reference. The absorbance was corrected by subtracting the background absorbance of control wells (medium and MTS reagent). DMSO treatment alone and untreated cells were used as negative controls, while 300 μM hydrogen peroxide (Acros Organics, NJ) was used as a positive control. Cell viability is expressed as a percentage of DMSO-treated cells. Each data point represents the average of three replicates.

3.5.4. Generation of dose–response curves and determination of CC_{50}

The data from the MTS assay were plotted as dose–response curves. The 50% cytotoxic concentration (CC_{50}) was determined from a linear regression of the data points surrounding 50% cell viability as described previously.[42] The data were normalized as described above. Briefly, data were normalized by subtracting from each experimental value the average percentage of dead cells from six wells treated with 1% DMSO (solvent control). The two cellular viability percentages closest to the 50% value were plotted with its associated chemical compound concentration and the equation of the regression line was utilized to determine the CC_{50}.[42]

3.5.5. Apoptosis assay

For apoptosis assays, Ficoll-Paque™PLUS density gradient centrifugation[50,69] was used to increase the viability of Jurkat cells; this was done one day prior to the assay. Cells were centrifuged at 400×g for 30 min at room temperature and live cells at the interface were then collected and washed with cell culture medium. The resulting Jurkat cells were seeded in flat-bottomed 96-well MICROTEST™ plates at a cell density of 25,000 cells per well in 200 μL RPMI medium supplemented with 10% FBS and antibiotics as described above. **5b**, **5c**, **5g**, OTG, H_2O_2 (300 μM, apoptosis positive control), and Tween 20 (0.5%, necrosis positive control) were added to cells in triplicate at their CC_{50}. DMSO vehicle control and untreated cells, also in triplicate, were used as negative controls. Following 20 h of incubation, the cells were prepared for flow cytometry as previously described with minor modifications [39]). Briefly, ice-cold cells were centrifuged at 1400 rpm (357×g) for 5 min at 4 °C. The cells were then stained by resuspension in 100 μl binding buffer (0.1 M HEPES, pH 7.4, 140 mM NaCl, and 2.55 mM $CaCl_2$) containing 1 μl of 25 μg/ml annexin V-FITC and 5 μl of 250 μg/ml PI (Beckman Coulter, Miami, FL). Following 15

min of incubation on ice in the dark, 200 µl binding buffer was added. The cells were gently homogenized and analyzed using a Cytomics FC 500 flow cytometer (Beckman Coulter, Miami, FL), previously calibrated using unstained, single- (PI or annexin V-FITC) and double- (annexin V-FITC and PI) stained cells. For each sample, 3000 individual events were collected and analyzed using CXP software (Beckman Coulter, Miami, FL, USA).

3.6. Langmuir monolayer experiments

All experiments were performed on a Langmuir–Blodgett apparatus (Minitrough System 4, KSV Instruments Ltd., Finland) with a Teflon-coated trough (782 × 75 × 5 mm) and two hydrophilic Delrin barriers that were compressed symmetrically. The surface pressure was measured by the Wilhelmy plate method using a platinum plate (perimeter: 39.24 mm; height 10 mm). The subphase consisted of 150 mM NaCl, 1.5 mM $CaCl_2$ dihydrate on purified water. After pouring of the subphase, the temperature of the trough was adjusted via an external circulating bath. The barriers were compressed and surface-active impurities removed from the air–water interface with vacuum. The surfactant (50 µL of a 1.662 mM solution in dichlormethane/methanol = 9:1, *v*/*v*) was slowly spread over the subphase. The solvents were allowed to evaporate before the barriers were compressed at a constant speed of 10 mm/min (7.5 cm^2/min). Limiting molecular areas were calculated by extrapolating the linear region of the isotherm in the solid phase to zero surface pressure.

Acknowledgements

This work was supported by the National Science Foundation (CBET-0967381/0967390), the U.S. Department of Agriculture Biomass Research and Development Initiative (Grant Agreement 68-3A75-7-608) and the Department of Energy Development and Independence, Energy and Environment Cabinet of The Commonwealth of Kentucky. The cell culture work was performed at the Cell Culture Core of the Border Biomedical Research Center (BBRC) supported by grant 8G12MD007592 from the National Center for Research Resources (NCRR) of the NIH, granted to the University of Texas at El Paso.

References

1. Hill, K.; LeHen-Ferrenbach, C. In *Sugar-based surfactants: Fundamentals and Applications*; Ruiz, C. C., Ed.; CRC Press: Boca Raton, FL, 2009.
2. Kim, J.-H.; Block, D.; Mills, D. *Appl. Microbiol. Biotechnol.* **2010**, *88*, 1077–1085.
3. Prakash, G.; Varma, A. J.; Prabhune, A.; Shouche, Y.; Rao, M. *Bioresour. Technol.* **2011**, *102*, 3304–3308.
4. Sun, R.; Lawther, J. M.; Banks, W. B. *Ind. Crop Prod.* **1995**, *4*, 127–145.
5. Damez, C.; Bouquillon, S.; Harakat, D.; Henin, F.; Muzart, J.; Pezron, I.; Komunjer, L. *Carbohydr. Res.* **2007**, *342*, 154–162.
6. Bouxin, F.; Marinkovic, S.; Bras, J. L.; Estrine, B. *Carbohydr. Res.* **2010**, *345*, 2469–2473.
7. Matsumura, S.; Sakiyama, K.; Toshima, K. *Biotechnol. Lett.* **1999**, *21*, 17–22.
8. Xu, W.; Osei-Prempeh, G.; Lema, C.; Oldham, E. D.; Aguilera, R. J.; Parkin, S.; Rankin, S. E.; Knutson, B. L.; Lehmler, H. J. *Carbohydr. Res.* **2012**, *349*, 12–23.
9. Moses, J. E.; Moorhouse, A. D. *Chem. Soc. Rev.* **2007**, *36*, 1249–1262.
10. O'Neil, E. J.; DiVittorio, K. M.; Smith, B. D. *Org. Lett.* **2006**, *9*, 199–202.
11. Neto, V.; Granet, R.; Mackenzie, G.; Krausz, P. J. *Carbohydr. Chem.* **2008**, *27*, 231–237.
12. Read, R. W.; Wang, X. B. *Chiang Mai J. Sci.* **2009**, *36*, 247–257.
13. Read, R. W.; Wang, X. B. *J. Fluorine Chem.* **2012**, *135*, 25–32.
14. Paul, K. J. V.; Loganathan, D. *Tetrahedron Lett.* **2008**, *49*, 6356–6359.
15. Sani, F. A.; Heidelberg, T.; Hashim, R.; Farhanullah *Colloids Surf. B* **2012**, *97*, 196–200.
16. Lu, W.-Y.; Sun, X.-W.; Zhu, C.; Xu, J.-H.; Lin, G.-Q. *Tetrahedron* **2010**, *66*, 750–757.
17. Clemente, M. J.; Fitremann, J.; Mauzac, M.; Serrano, J. L.; Oriol, L. *Langmuir* **2011**, *27*, 15236–15247.
18. Rostovtsev, V. V.; Green, L. G.; Fokin, V. V.; Sharpless, K. B. *Angew. Chem.* **2002**, *114*, 2708–2711.
19. Li, X.; Turánek, J.; Knötigová, P.; Kudláčková, H.; Mašek, J.; Parkin, S.; Rankin, S. E.; Knutson, B. L.; Lehmler, H.-J. *Colloids Surf. B* **2009**, *73*, 65–74.
20. Li, X.; Turanek, J.; Knotigova, P.; Kudlackova, H.; Masek, J.; Pennington, D. B.; Rankin, S. E.; Knutson, B. L.; Lehmler, H.-J. *New J. Chem.* **2008**, *32*, 2169–2179.
21. Gruzman, A.; Shamni, O.; BenYakir, M.; Sandovski, D.; Elgart, A.; Alpert, E.; Cohen, G.; Hoffman, A.; Katzhendler, Y.; Cerasi, E.; Sasson, S. *J. Med. Chem.* **2008**, *51*, 8096–8108.
22. Zinner, H.; Nimz, H. *Naturwissenschaften* **1959**, *46*, 531–532.
23. Rowan, A. S.; Nicely, N. I.; Cochrane, N.; Wlassoff, W. A.; Claiborne, A.; Hamilton, C. J. *Org. Biomol. Chem.* **2009**, *7*, 4029–4036.
24. Alvarez, S. G.; Alvarez, M. T. *Synthesis* **1997**, *1997*(413), 414.
25. Chambert, S.; Doutheau, A.; Queneau, Y.; Cowling, S. J.; Goodby, J. W.; Mackenzie, G. *J. Carbohydr. Chem.* **2007**, *26*, 27–39.
26. Goodby, J. W.; Haley, J. A.; Watson, M. J.; Mackenzie, G.; Kelly, S. M.; Letellier, P. *Liq. Cryst.* **1997**, *22*, 497–508.
27. Harmouch, B.; Gode, P.; Goethals, G.; Goodby, J.; Haley, J.; Kelly, S.; Letellier, P.; Mackenzie, G.; Martin, P.; Ronco, G.; Watson, M.; Villa, P. *J. Carbohydr. Chem.* **1997**, *16*, 479–497.
28. Donnio, B.; Seddon, J. M.; Deschenaux, R. *Organometallics* **2000**, *19*, 3077–3081.
29. Galema, S. A.; Engberts, J. B. F. N.; Van Doren, H. A. *Carbohydr. Res.* **1997**, *303*, 423–434.
30. Goodby, J. W. *Liq. Cryst.* **1998**, *24*, 25–38.
31. Goodby, J. W.; Gortz, V.; Cowling, S. J.; Mackenzie, G.; Martin, P.; Plusquellec, D.; Benvegnu, T.; Boullanger, P.; Lafont, D.; Queneau, Y.; Chambert, S.; Fitremann, J. *Chem. Soc. Rev.* **2007**, *36*, 1971–2032.
32. Prade, H.; Miethchen, R.; Vill, V. *J. Prakt. Chem.-Chem. Ztg.* **1995**, *337*, 427–440.
33. Noller, C. R.; Rockwell, W. C. *J. Am. Chem. Soc.* **1938**, *60*, 2076–2077.
34. Goodby, J. W.; Marcus, M. A.; Chin, E.; Finn, P. L.; Pfannemuller, B. *Liq. Cryst.* **1988**, *3*, 1569–1581.
35. Söderlind, E.; Wollbratt, M.; von Corswant, C. *Int. J. Pharm.* **2003**, *252*, 61–71.
36. Zarif, L.; Greiner, J.; Pace, S.; Riess, J. G. *J. Med. Chem.* **1990**, *33*, 1262–1269.
37. Deyrieux, A.; Wilson, V. G. *Cytotechnology* **2007**, *54*, 77–83.
38. Martínez, A.; Rajapakse, C. S. K.; Sánchez-Delgado, R. A.; Varela-Ramirez, A.; Lema, C.; Aguilera, R. J. *J. Inorg. Biochem.* **2010**, *104*, 967–977.
39. Shaik, N.; Martínez, A.; Augustin, I.; Giovinazzo, H.; Varela-Ramírez, A.; Sanaú, M.; Aguilera, R. J.; Contel, M. *Inorg. Chem.* **2009**, *48*, 1577–1587.
40. Pavillard, V.; Drbal, A. A. A.; Swaine, D. J.; Phillips, R. M.; Double, J. A.; Nicolaou, A. *Biochem. Pharmacol.* **2004**, *67*, 1587–1599.
41. Kolb, H. C.; Sharpless, K. B. *Drug Discovery Today* **2003**, *8*, 1128–1137.
42. Varela-Ramirez, A.; Costanzo, M.; Carrasco, Y.; Pannell, K.; Aguilera, R. *Cell Biol. Toxicol.* **2011**, *27*, 159–168.
43. Balgavý, P.; Devínsky, F. *Adv. Colloid Interface Sci.* **1996**, *66*, 23–63.
44. Devínsky, F.; Kopecka-Leitmanová, A.; Šeršeň, F.; Balgavý, P. *J. Pharm. Pharmacol.* **1990**, *42*, 790–794.
45. Mlynarcik, D.; Denyer, S. P.; Hugo, W. B. *Microbios* **1981**, *30*, 27–35.
46. Kamp, F.; Hamilton, J. A. *Prostaglandins Leukot. Essent. Fatty Acids* **2006**, *75*, 149–159.
47. Milius, A.; Greiner, J.; Riess, J. G. *New J. Chem.* **1992**, *16*, 771–773.
48. Zarif, L.; Greiner, J.; Riess, J. G. *J. Fluorine Chem.* **1989**, *44*, 73–85.
49. Mukerjee, P. *J. Am. Oil Chem. Soc.* **1982**, *59*, 573–578.
50. Miyoshi, N.; Oubrahim, H.; Chock, P. B.; Stadtman, E. R. *Proc. Natl. Acad. Sci. USA* **2006**, *103*, 1727–1731.
51. Wang, Y.; Jin, Y. *Toxicol. Res.* **2012**, *1*, 103–107.
52. Li, X.-Y.; Jing, C.-Q.; Lei, W.-L.; Li, J.; Wang, J.-J. *Ecotoxicol. Environ. Saf.* **2012**, *83*, 102–107.
53. Oldham, E. D.; Xie, W.; Farnoud, A. M.; Fiegel, J.; Lehmler, H. J. *J. Phys. Chem. B* **2012**, *116*, 9999–10007.
54. Nielson, D. W. *J. Appl. Physiol.* **1986**, *60*, 972–979.
55. Cea, P.; Martín, S.; Villares, A.; Möbius, D.; López, M. C. *J. Phys. Chem. B* **2005**, *110*, 963–970.
56. Berg, J. M.; Eriksson, L. G. T. *Langmuir* **1994**, *10*, 1213–1224.
57. Tamada, K.; Minamikawa, H.; Hato, M.; Miyano, K. *Langmuir* **1996**, *12*, 1666–1674.
58. Lehmler, H.-J.; Fortis-Santiago, A.; Nauduri, D.; Bummer, P. M. *J. Lipid Res.* **2005**, *46*, 535–546.
59. Lehmler, H.-J.; Bummer, P. M. *J. Colloid Interface Sci.* **2002**, *249*, 381–387.
60. Vollhardt, D.; Siegel, S.; Cadenhead, D. A. *Langmuir* **2004**, *20*, 7670–7677.
61. Kellner, B. M. J.; Mullerlandau, F.; Cadenhead, D. A. *J. Colloid Interface Sci.* **1978**, *66*, 597–601.
62. Gaines, G. L. *Insoluble Monolayers at Liquid-Gas Interfaces*; Interscience Publishers: New York, 1966.
63. Boyd, B. J.; Drummond, C. J.; Krodkiewska, I.; Grieser, F. *Langmuir* **2000**, *16*, 7359–7367.
64. Boullanger, P.; Chevalier, Y. *Langmuir* **1996**, *12*, 1771–1776.
65. Garofalakis, G.; Murray, B. S. *Langmuir* **2002**, *18*, 4765–4774.
66. Frey, S. L.; Lee, K. Y. C. *Langmuir* **2007**, *23*, 2631–2637.
67. Kaganer, V. M.; Brezesinski, G.; Möhwald, H.; Howes, P. B.; Kjaer, K. *Phys. Rev. E* **1999**, *59*, 2141–2152.
68. Nguyen, D. M.; Miles, D. H. *Synth. Commun.* **2011**, *41*, 1759–1771.
69. Boyum, A. *Scand. J. Clin. Lab. Invest. Suppl.* **1968**, *97*, 77–89.